Computational Fluid Dynamics Modeling of Macro-Meso Porous Monoliths for Continous Catalysis

By

Tahir Mahmood Ahmed

School of Chemical and Materials Engineering

National University of Sciences and Technology

2022

Computational Fluid Dynamics Modeling of Macro-Meso Porous Monoliths for Continous Catalysis

Name: Tahir Mahmood Ahmed

Reg No: 00000359759

This work is submitted as an M.S. thesis in partial fulfillment of the requirement for the degree of

M.S. in Process Systems Engineering

Supervisor Name: Dr. Sher Ahmad

School of Chemical and Materials Engineering (SCME)
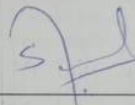
National University of Sciences and Technology (NUST)

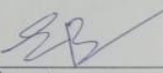**H-12 Islamabad, Pakistan**

August 2023

THESIS ACCEPTANCE CERTIFICATE

Certified that final copy of MS thesis written by Mr **Tahir Mahmood Ahmad** (Registration No 00000359759), of School of Chemical & Materials Engineering (SCME) has been vetted by undersigned, found complete in all respects as per NUST Statues/Regulations, is free of plagiarism, errors, and mistakes and is accepted as partial fulfillment for award of MS degree. It is further certified that necessary amendments as pointed out by GEC members of the scholar have also been incorporated in the said thesis.
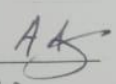
Signature: _____

Name of Supervisor: **Dr Sher Ahmad**

Date: 11/10/23

Signature (HOD): _____

Date: 11/10/23

Signature (Dean/Principal): _____

Date: 11.10.20 23

Form TH-1

National University of Sciences & Technology (NUST)
MASTER'S THESIS WORK
Formulation of Guidance and Examination Committee

Name: **Tahir Mahmood Ahmed**

Department: **SCME**

Credit Hour Completed (21) 24

NUST Regn No: **00000359759**

Specialization: Process Systems Engineering

CGPA (3.29) 3.38

Course Work Completed

S/No	Code	Title	Core/Elective	CH	Grade
1	PSE-801	Process System Theory	Core	03	B+
2	PSE-852	Process Modeling and Simulation	Core	03	B
3	PSE-802	Optimization and Decision Analysis	Core	03	B+
4	PSE-823	Advance Process Dynamics & Controls	Core	03	B+
5	TEE-820	Process Intensification	Elective	03	B+
6 CSE	SCE-801	Computational Fluid Dynamic	Elective	03	B
7	ENE-809	Waste Water Treatment	Elective	03	B
✗ 8	CHE-814	Product Technology	Elective	03	A

Date 01-03-2022

Student's Signature _____

Thesis Committee

1. Name: **Dr. Sher Ahmad (Supervisor)**
   Department: Chemical Engineering

   Signature: _____

2. Name: **Dr. Muhammad Ahsan (Co-Supervisor)**
   Department: Chemical Engineering

   Signature: _____

3. Name: **Dr. Iftikhar Ahmad**
   Department: Chemical Engineering

   Signature: _____

4. Name: **Dr. Nouman Ahmad**
   Department: Chemical Engineering

   Signature: _____

Date: 29/3/22

Signature of Head of Department: _____

APPROVAL

Date: 29-3-2022

Dean/Principal _____

Distribution
1x copy to Exam Branch, HQ NUST
1x copy to PGP Dte, HQ NUST
1x copy to Exam branch, respective institute

School of Chemical and Materials Engineering (SCME) Sector H-12, Islamabad

✗ 9. RM-898 Research methodology Additional 2 Q

National University of Sciences &Technology (NUST)

MASTER'S THESIS WORK

We hereby recommend that the dissertation prepared under our supervision by

Regn No & Name: 00000359759 Tahir Mahmood Ahmed

Title: Computational Fluid Dynamics Modeling of Macro-Meso Porous Monoliths for Continuous Catalysis.

Presented on: 28 Sep 2023   at: 1500 hrs in SCME (Seminar Hall)

Be accepted in partial fulfillment of the requirements for the award of Master of Science degree in **Process Systems Engineering**.

Guidance & Examination Committee Members

Name: **Dr Iftikhar Ahmad**   Signature:

Name: **Dr Nouman Ahmad**   Signature:

Name: **Dr Muhammad Ahsan** (Co-Supervisor)   Signature:

Supervisor's Name: **Dr Sher Ahmad**   Signature:

Dated: 05|10|23

Head of Department
Date 10|10|23

Dean/Principal
Date   10.10.20 23

School of Chemical &Materials Engineering (SCME)

I have devoted my thesis to my family constant support,

encouragement, love, and honour.

Acknowledgment

All praise and eminence are due to "ALLAH," the undisputed architect of this world, who gave us the capacity for comprehension and sparked our curiosity about the planet as a whole. Warmest welcomes to the supreme ruler of this world and the hereafter, "Prophet Mohammed (PBUH)," a source of knowledge and benefits for all of humanity as well as for Uma.

I would like to acknowledge and express my sincere gratitude to my research **supervisor**, **Dr. Sher Ahmad** for his endless support, supervision and affectionate guidance to steer me in the right the direction whenever he thought I needed it. I would also like to extend my gratitude to my **co-supervisor Dr. Ahsan**, **committee members**; **Dr. Iftikhar Ahmad** and **Dr. Nouman Ahmad**. for their valuable suggestions and guidance.

I would also like to thank **Prof. Dr. Amir Azam Khan** (Principal School of Chemical and Materials Engineering) and **Dr. Erum Pervaiz** (HOD Department of Chemical Engineering) for providing a research oriented platform to effectively utilize my skills in accomplishing this research work.

In the end, I must express my very profound gratitude to my parents for providing me with unfailing support and continuous encouragement throughout my years of study and through the process of researching and writing this thesis. This accomplishment would not have been possible without them.

Tahir Mahmood Ahmed

Abstract

In this study, a 2D axisymmetric homogenized monolith geometry was utilized to develop a CFD model, which was then applied to investigate the heterogeneous catalyzed Knoevenagel condensation reaction. The CFD model encompasses convective fluid flow in the macro pores, species diffusion, and reaction kinetics in the meso pores of the monolith. The model's accuracy was affirmed through successful validation against previously available experimental data in the literature for the Knoevenagel condensation reaction.

Subsequently, the model was employed to examine the influence of key parameters, such as meso and macroporosity, on flow and diffusion. Moreover, reaction parameters, including temperature and multiscale reactor size, were explored, ranging from the pore level to the reactor length.

To analyze flow patterns and concentration profiles at the macro pore level, pore-scale simulations were conducted through image processing and CFD modeling of 25x25 µm Scanning Electron Microscopy (SEM) images of the porous monoliths. These simulations yielded an in-depth comprehension of pore flow and concentration behaviors at the macro-meso level, offering valuable insights for optimizing pores in hierarchical structures.

Keywords: Computational Fluid Dynamics (CFD), monolith**,** heterogeneous, Scanning Electron Microscopy (SEM), axisymmetric, homogenized, Knoevenagel condensation.

Table of Contents

List of Figures

List of Tables

Nomenclature

CFD	Computational Fluid Dynamics
SEM	Scanning Electron Microscopy
HPSLC	High Pressure solid Liquid catalysis
HPLC	High performance liquid chromatography
CA	Cellulose acetate
MN	Monolith
VAPM	volume averaged porous medium
3D	3-Dimensional
CPM	Classical porous medium
SMR	steam methane reforming
2D	2-Dimensional
ECA	Ethyl cyanoacetate
BA	Benzaldehyde
ECC	Ethyl trans-α-cyanocinnamate
R_i	reaction rate
c_t	concentration at time 't'
c_o	initial concentration
A	pre-exponential factor
E_a	activation energy
T	reaction temperature
φ_B	association factor
M_B	Molecular weight of ethanol
μ_B	dynamic viscosity of ethanol
$v_{b,A}$	Molar volume of Ethyl cyanoacetate
k	rate constant
R	universal gas constant
$D_{D,i}$ (D_{AB})	Diffusivity of reactant ECA in ethanol
ε_{macro}	macro porosity
ε_{meso}	meso porosity

τ_{meso}	meso pore space tortuosity
ε_{total}	total porosity
K_d	hydraulic permeability
J_i	total flux
$D_{e,i}$	effective diffusivity
c_i	species concentration
μ	dynamic viscosity of the fluid
u	velocity vector
P	pressure
κ	permeability of the porous medium

Chapter 1

Introduction

1.1 Background

Catalysis is of crucial importance for chemical, petrochemical, petroleum refining, energy and environmental sectors [1]. Catalyst molecules may induce the transformation of many molecules of reactents. Continuous-flow catalytic processes provide sustainable long term production of fine chemical compounds [2]. These processes have significant advantages over the batch reactions in terms of productivity, resource efficiency and environmental protection [3,4].

Homogenous catalysts such as amino acids, ammonium salts, amines and organometallic catalysts [5,6,7,8] have several shortcomings like product separation, catalyst recovery, large volume of waste generation and high reaction temperatures. Heterogeneous catalysts such as metal organic framework, zeolites, ionic liquids, functionalized mesoporous silica have been successfully developed and employed in order to overcome these shortcomings for the synthesis of fine chemicals [9].

The porous catalyst supports in heterogeneous catalysis reduces the pore size providing a large surface area for faster reaction kinetics. However, the increase in surface area constricts the flow path length of the reacting species resulting in an increase in an overall pressure drop. So there is interplay between surface area and flow path length, hence such porous catalyst supports are required that can help to achieve a uniform residence time and faster kinetics in the porous reactors.

Macro meso porous monoliths are rigid support structures with hierarchical interconnected porous network [10,11,12]. Macro pores(>50 nm) allow transport by convection through the porous material, meso pores (2−50 nm) are accessible through diffusion and thus provide a large surface area for reaction kinetics [11]. They have low pressure drop, high mass transfer rate, small diffusion lengths and thermal stability over conventional catalyst pellets [13,14]. They have been implemented in many catalytic reactions such as Diels-Alder reaction [15], Friedlander reaction [3], selective hydrogenation[16], and Knoevenagel condensation reaction [17].

Mathematical modeling provides an understanding of several dynamic processes in many industrial applications [18]. Flow and transport phenomenon in porous reactors can be explained by either pore scale or macroscopic (Darcy scale) models. Pore scale simulations employ Stokes equations for the fluid flow and Fick's law of diffusion for the solute transport, but it needs the knowledge of pore geometry that is rarely available. The heterogeneity of porous media, lack of detailed information about the pore geometry of porous media and the high computational cost makes it impractical for the pore scale modeling [19].

Macroscopic models which treat the porous media as an "average" continuum are employed to overcome these limitations [19]. The up scaling from the pore scale to macro scale is carried out by several mathematical approaches such as volume averaging [20], thermodynamically constrained averaging theory [21], pore-network models [22], and the homogenization [23,24].

Homogenization is a macro scale modeling approach that is applied to solve the differential equations of the physical phenomena in a heterogeneous porous domain at the two scales to obtain a locally averaged domain [25]. The homogenization approach is the replacement of the heterogeneous porous medium by an equivalent homogeneous medium. Therefore, it is a method to study the macroscopic behavior of a porous medium by its microscopic properties [26].

The homogenized medium is described by the effective coefficients and it need a periodic assumption [27]. This spatially periodic assumption makes it possible for the averaging of the micro scale effects to produce macroscopic properties. The up scaled models that result by applying these techniques are written usually in the form of effective coefficients [28]. These coefficients can be determined by solving the ancillary closure problems based on the periodic representations of the micro structure of the porous medium. These calculated coefficients determine the transport phenomenon from the pore scale to the macroscopic level of the porous medium [28]. Over the last few decades modeling and simulation has gained importance in general and Computational fluid dynamics (CFD) modeling and simulation in particular for engineering applications.

CFD is a powerful modeling and simulation tool used in many industrial processes [29]. It provides deep insights into the dynamic properties such as temperatures,

pressures and compositions within a reactor which are mandatory to the catalytic performance [30]. It is related to the fluids in motion, which physical characteristics can be explained through modeling equations [29,31].

This research work presents the development of CFD homogenized model aimed at understanding the application of monoliths for heterogeneous catalysis. The novelty of work is that we have developed a CFD homogenized model and proposed up scaling from pore scale to macroscopic level. Most important of all is that we have taken actual SEM data and performed pore scale SEM CFD modeling by coupling flow with transport phenomenon

1.2 Objectives

The objectives of the thesis are given below,

- Development of the homogenized CFD model for macro-meso porous monoliths for heterogeneous catalysis.
- Development of the pore scale SEM CFD model.
- Coupling of fluid behaviour with reaction kinetics in porous monoliths.
- Effects of structural parameters on reaction conversion.

1.3 Thesis Outline

The thesis is organized as follows. Chapter 1 describes the background, followed by chapter 2, which gives a detailed literature review. Chapter 3 discusses the research methodology to develop the macro meso porous monolith homogenized CFD model and SEM CFD modeling . Chapter 4 contains the simulation results, comparison of experimental and model simulation results leading to the model validation, discussions about the model significance, the structural effects on the conversion and the future prospects of the research work.

Chapter 2

Literature Review

2.1 Literature Review

Catalysis is an important field with majority of the industrial chemical processes involving the catalysts in at least one of their steps [32]. At present, because of productivity, catalyst separation and other environmental issues, catalysis appears to be more important than before and it constitute to be one of the major sources of industrial production and development [33,34].

Various studies based have been reported based on continuous flow catalysis, Knoevenagel condensation reaction in heterogeneous catalysis, mathematical modeling and CFD modeling of heterogeneous catalysis for porous reactors based on the macro scale techniques. For instance, Haas et al. [11] employed the macro meso porous amine-functionalized monoliths in the knoevegnal condensation reaction in heterogeneous catalysis to determine the intrinsic reaction kinetics. The reactor performance was online monitored using HPSLC–HPLC experimental configuration. The comparable properties for the kinetic studies of the Knoevenagel condensation were used to find out the activation energies.

Schulze et al. [35] immobilized DMAP organo catalyst on silica particles and monoliths for continuous flow. Silica monoliths exhibited lower pressure drop and a better conversion in comparison to the packed bed reactors. The turn over frequencies of silica monoliths came out to be 9.3×10^{-2} sec^{-1} twice the batch experiment. They proved to be a suitable catalyst support materials for organo catalysis.

Appaturi et al. [9] discussed the reaction process and the parameters involved in the condensation reaction. It discussed the use of heterogeneous catalysts such as in the metal oxides, mesoporous silica, zeolites, ionic liquids, carbon nitride-based catalysts for the Knoevenagel condensation reaction. It proposed that for meso porous catalyst system having multiple properties is mandatory to build a zero waste efficient system.

Sachse et al. [36] used Al-MonoSil as catalytic micro reactor in the implementation of Diels–Alder reaction. It showed in continuous flow high conversion and productivity with a little pressure drop (<0.5 bar) and hence proved to be a stable micro reactor.

Linares et al. [2] immobilized Pd nanoparticles on dual porous titania monoliths by a green procedure. This catalytic setup was used in continuous flow catalytic hydrogenation reactions with excellent durability, selectivity and efficiency. It showed outstanding performance in continuous partial hydrogenation process under mild conditions. The reason for such a performance is the dual porous structure of monolith. The monolith provides a good residence time, low pressure drop and a high rate of mass transfer through the catalytic material.

Turke et al. [37] reported the application of immobilized(3-aminopropyl) trimethoxysilane (APTMS) silica monoliths in heterogeneous catalysis. The reaction considered was continuous Knoevenagel condensation between various aromatic aldehydes and cyano ethylacetate. The silica monoliths showed a high conversion of 95% with concurrent minimum back pressure. High conversion can be maintained by connecting two monoliths having different meso pore sizes.

Xiao et al. [38] developed a monolith bio reactor by lipase immobilization on Cellulose acetate CA monolith (CA-MN). More than 90% conversion in continuous esterification/ trans-esterification reaction in the monolith bio reactor because of the macro meso porous structure of the CA monolith.

Battiato et al. [27] presented up scaling methods that are used to derive equations based on macro scale from pore scale level. This review study included the mixture theory, volume averaging method, thermodynamically constrained averaging, renormalization group techniques and homogenization. The basic purpose of this review article was to provide the knowledge about the principles these methods are based upon, their specific advantages and shortcomings

Kavale et al. [39] developed a volume averaged porous medium (VAPM) CFD monolith model to calculate the catalytic reaction rates. The VAPM model was validated against the experiments of the steam methane reforming in a catalytic monolith. The developed methodology was assessed against fully resolved 3D multichannel monolith simulations. The VAPM approach was compared to the

classical porous medium (CPM) approach for CO oxidation and CO_2 to methanol conversion. The detailed simulations and VAPM model results were not in agreement on the conversion results so there is a need to accurately evaluate the reaction kinetics.

Dixon [40] developed a 3D CFD model and performed particle resolved simulations (PR) for a packed bed. The model coupled the reaction kinetics with the transport and the fluid flow phenomenon for the steam methane reforming (SMR) process.

Paterea et al. [41] presented a two finite element mesh system by coupling micro and macro geometries. The method was applied to industrial fixed bed reactor in the synthesis of methanol; however the concentration results were not in a good agreement with the experimental findings.

Sadeghi et al. [42] developed a steady state frame work that was based on pore network modeling. The reactive transport was analyzed inside a single 2D porous particle under steady state conditions. A parametric study was carried out in terms of reaction rate to determine the effects of structural parameters on the particle performance. The lower pore size particle was less reactive at constant macro porosity. The optimum catalyst particle structure was evaluated to be nano porous to mostly macro porous on reactivity.

Ghouse and Adams [43] developed a two-dimensional, heterogeneous model for catalytic steam methane reforming (SMR). It was observed that in gas solid heterogeneous systems diffusional limitations can be accounted with accuracy without using the effectiveness factor a specific catalyst.

Bai et al. [44] provided the simulation results of the pressure drop and the fluid flow in a randomly catalyst packed fixed-bed reactor. The model simulation results showed deviation from the experimental findings with increase in the gas flow rate.

Dixon and Nijemeisland [45] presented CFD as a designing tool for the packed bed reactors. The gas flow was simulated in catalyst particles and thus it provided accurate information about the flow fields.

Shi et al. [46] described that the pore structure plays an important role in the design and optimization of hierarchically structured HDM catalysts. The results indicated that that adjusting macro pore diameter is an effective way to reduce the diffusion

limitations. It also described that the reaction only takes place in the meso pores of the catalyst pellets as it provides higher surface area with more active sites, and also that a smaller meso pore diameter gives rise to a steeper concentration gradient.

Meyers and Liapis, Tallarek et al. & Jungreuthmayer et al. [47,10,48] developed techniques based on the macro structure to evaluate the velocity profile, diffusion and species transport through the porous monolith medium. These approaches were costly, time consuming and required high computation.

Sadeghi et al. [42] developed a steady state frame work that was based on pore network modeling. The reactive transport was analyzed inside a single 2D porous particle under steady state conditions. A parametric study was carried out in terms of reaction rate to determine the effects of structural parameters on the particle performance. The lower pore size particle was less reactive at constant macro porosity. The optimum catalyst particle structure was evaluated to be nano porous to mostly macro porous on reactivity.

Potter et al. [30] developed a 2D CFD-catalysis porous media model that provided insights into the temperature, mole fraction and local concentration of reactants and products for the dehydration of ethanol into ethylene, using a fixed-bed reactor. However, there is a need to implement more porous scale averaging models which can enhance the potential to more active sites accessibility and hence finally increase the conversion and productivity.

Although numerous research studies have been published on the CFD modeling of porous reactors but no work is reported on the homogenized CFD modeling of macro meso porous monoliths employed for the Knoevenagel condensation of Benzaldehyde and Ethyl cyanoacetate with Ethanol as a solvent to produce Ethyl trans-α-cyanocinnamate. Furthermore, no work has been done on SEM CFD modeling by coupling flow with transport phenomenon.

Chapter 3

Process Description and Methodology

3.1 Process Description

3.1.1 Experimental set up for Knoevenagel condensation

To develop the CFD model, a case study of silica based monolithic continuous flow micro reactor for Knoevenagel condensation reaction is taken from previously published literature [11]. The experimental setup consists of reactants ECA and BA being mixed in the micro mixer and then fed into the monolithic reactor having length of 100 mm and a diameter of 4.6 mm. as shown in figure 1:
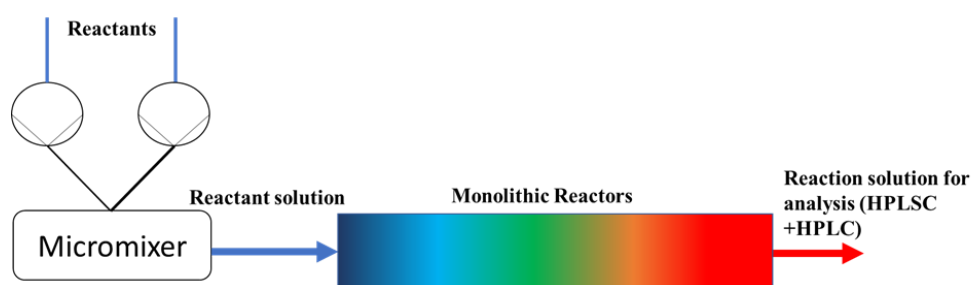
Figure 1: Experimental setup for the Knoevenagel condensation reaction

During Knoevenagel condensation reaction carbon-carbon bond formation processes in the synthesis of organic compounds in which between benzaldehyde (BA) and ethyl cyanoacetate (ECA) with ethanol as a solvent reacts in a silica based monolithic continuous flow micro reactor to produce ethyl trans-α-cyanocinnamate (ECC) according to the Eq (1):

$$BA + ECA \xrightarrow[\substack{10\text{-}40°C}]{EtOH} ECC + H_2O \qquad (1)$$
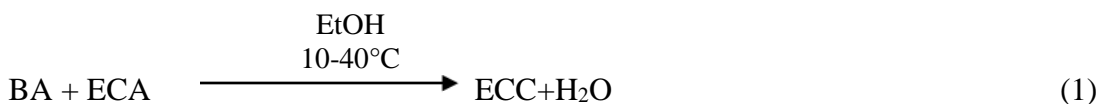
The rate of the reaction is expressed in terms of ECC concentration as given in Eq (2).

$$R_i = \frac{dc(ECC)}{dt_{rct}} = kc_t(ECA)^n c_t(BA)^m \qquad (2)$$

Where k is the reaction rate coefficient, c_t is the concentration at time 't', variables n and m indicate the reaction order with respect to ECA and BA. The initial rate is nearly unchanged with increasing (c_o BA)/(c_o ECA) for excess amount of BA

keeping the initial concentration c_o(ECA) constant. So the reaction order with respect to BA becomes m=0 in Eq (2), the overall reaction order is first order (n=1) with respect to ECA and the reaction rate can be written as [11]:

$$R_i = \frac{dc(ECC)}{dt_{rct}} = kc_t(ECA) \qquad (3)$$

The rate constant 'k' is temperature dependent and is calculated from Arrhenius equation, Eq (4):

$$k = Ae^{-\frac{E_a}{RT}} \qquad (4)$$

Where 'k' is the reaction rate coefficient, 'A' is the pre-exponential factor, 'R' is the universal gas constant, E_a is the activation energy of the Knoevenagel reaction and 'T' is the reaction temperature

The Diffusivity of reactant ECA in pure ethanol solution was calculated using Wilke-Chang Equation, Eq (5):

$$D_{D,i} = D_{AB} = 7.4 \times 10^{-8} \frac{(\varphi_B M_B)^{0.5} T}{v_{b,A}^{0.6} \mu_B} \qquad (5)$$

In eq. 5, subscript A represent ECA, B represents Pure Ethanol. For Ethanol φ_B = association factor, M_B = Molecular weight of ethanol, μ_B dynamic viscosity of ethanol, $v_{b,A}$ = Molar volume

Whereas the molar volume is calculated as:

$$v_{b,A} = 7.047 + 0.4v_{c,A} + (0.01724 + \frac{15.37}{T_{c,A}} + 0.00438\omega_A)T_{b,A} \qquad (6)$$

The dynamic viscosity of ethanol is calculated by the equation:

$$\mu_B = \exp(-6.21 + \frac{1614}{T} + 0.00618T - 1.132 \times 10^{-5}T^2) \qquad (7)$$

3.2 Methodology

Figure 2 shows the methodology followed in developing CFD homogenized model for macro meso porous monolith and SEM CFD modeling
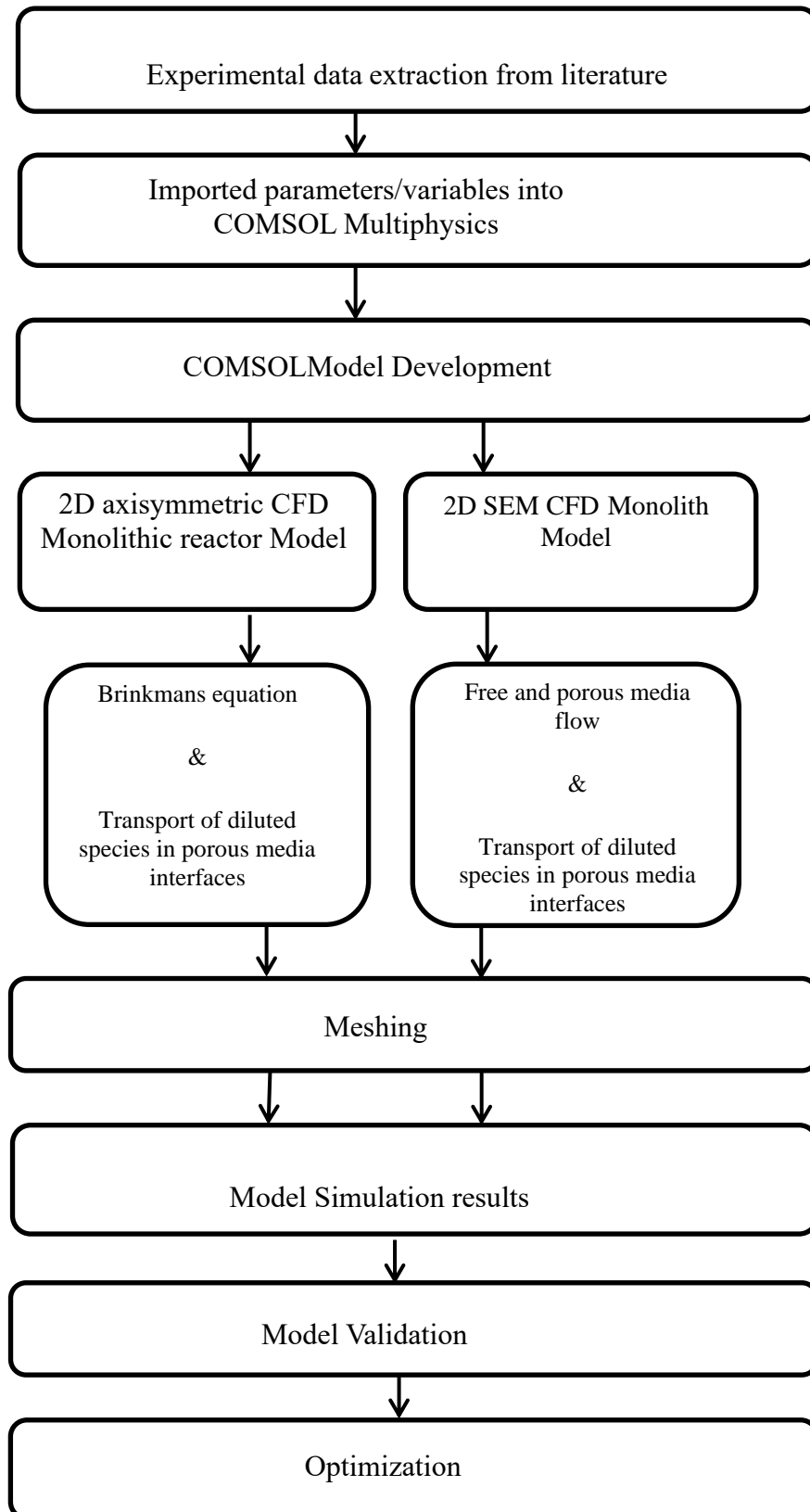
```
┌─────────────────────────────────────────────────────────────────┐
│        Experimental data extraction from literature               │
└─────────────────────────────────────────────────────────────────┘
                              │
                              ▼
┌─────────────────────────────────────────────────────────────────┐
│              Imported parameters/variables into                    │
│                   COMSOL Multiphysics                             │
└─────────────────────────────────────────────────────────────────┘
                              │
                              ▼
┌─────────────────────────────────────────────────────────────────┐
│                 COMSOLModel Development                            │
└─────────────────────────────────────────────────────────────────┘
              │                            │
              ▼                            ▼
┌────────────────────────┐    ┌────────────────────────┐
│ 2D axisymmetric CFD     │    │ 2D SEM CFD Monolith     │
│ Monolithic reactor Model│    │ Model                   │
└────────────────────────┘    └────────────────────────┘
              │                            │
              ▼                            ▼
┌────────────────────────┐    ┌────────────────────────┐
│ Brinkmans equation      │    │ Free and porous media   │
│                         │    │ flow                    │
│         &               │    │                         │
│                         │    │         &               │
│ Transport of diluted    │    │                         │
│ species in porous media │    │ Transport of diluted    │
│ interfaces              │    │ species in porous media │
│                         │    │ interfaces              │
└────────────────────────┘    └────────────────────────┘
              │                            │
              ▼                            ▼
┌─────────────────────────────────────────────────────────────────┐
│                          Meshing                                  │
└─────────────────────────────────────────────────────────────────┘
              │                            │
              ▼                            ▼
┌─────────────────────────────────────────────────────────────────┐
│                  Model Simulation results                         │
└─────────────────────────────────────────────────────────────────┘
                              │
                              ▼
┌─────────────────────────────────────────────────────────────────┐
│                     Model Validation                              │
└─────────────────────────────────────────────────────────────────┘
                              │
                              ▼
┌─────────────────────────────────────────────────────────────────┐
│                       Optimization                                │
└─────────────────────────────────────────────────────────────────┘
```

Figure 2: Schematic of the homogenized CFD model & SEM Modeling in COMSOL

Multiphysics

3.3 Modeling in COMSOL MULTIPHYSICS

The steady state homogenized model was developed in COMSOL Multiphysics 5.6. The model was built using the transport of diluted species in porous media and the brinkman equations. The basic purpose of the model was to couple the reaction kinetics with transport phenomenon in a hierarchical monolithic structure. The modeling parameters molecular diffusion coefficients, effective diffusivity, permeability and reaction kinetics were taken from the experimental data [11].

3.3.1 Model Assumptions

The following assumptions were made for the development of the model:

•   Isothermal conditions within the reactor

•   Steady-state conditions within the reactor geometry

•   Homogenous porous structure

•   Plug flow conditions

•   Uniform flow and concentration distribution within the porous structure.

3.3.2 Homogenization

Homogenized approach consumes relatively less time and cost and is very effective technique to solve porous models which otherwise would require high computation cost and specialized techniques. The homogenization approach is useful to explain a continuous geometrical shape with repeating unit at micro-meso level, specifically a hierarchal porous structure geometry, which otherwise require high computational resources to compute. This approach is based on the idea to replace the micro-meso domains with repeating geometric details by an equivalent homogeneous domain, whose behavior represents the average behavior of the composite at macroscopic scale.

3.3.3 Model input parameters

The model input parameters were taken from the experimental setup from the Haas et al. [11] as shown in the table 1:

Table 1: Model building parameters used in COMSOL Multiphysics

Parameters	Value	Reference
Macro porosity (ε_{macro})	0.57	Taken from [11]
Meso porosity (ε_{meso})	0.68	
Meso pore space tortuosity (τ_{meso})	1.25	
Total porosity(ε_{total})	0.86	
K_d (monoliths)	$2.3*10^{-14}m^2$	
Monolith column dimensions	4.6mm(dia)*100mm(length)	
Initial concentration c_o(BA)	30 mmol L^{-1}	
Initial concentration c_o(ECA)	25 mmol L^{-1}	
Flow rate Q	0.2-3.5 ml min^{-1}	
Temperature Range	10-40°C	
Selected temperatures(for conversion)	10°C, 25°C,40°C	
Activation Energy Ea	30.4 KJ mol^{-1}	
Reaction Enthalpy	30400 J mol^{-1}	
R1(Universal gas constant)	8.314 J $mol^{-1}K^{-1}$	
Rate constant(298 K)	0.019162 s^{-1}	
Rate constant(313 K)	0.0345 s^{-1}	
Diffusivity of ECA in pure ethanol solution(283K)	5.72e-10 $m^2 s^{-1}$	Estimated from eq.5

Diffusivity of ECA in pure ethanol solution(298K)	8.08 e^{-10} m^{2}s^{-1}	Estimated from eq.5
Diffusivity of ECA in pure ethanol solution(313K)	1.11e–9 m^{2}s^{-1}	
Dynamic Viscosity(Ethanol)	1.39 cPa*s	Estimated from eq.7

3.4 CFD Modeling of Homogenized Macro Meso Porous Monolith

The macro-meso porous homogenized monolith model geometry was built in COMSOL Multiphysics in 2D-Axisymmetric dimensions using steady state conditions by coupling Brinkman flow and reaction kinetics. The objective of COMSOL model was to determine the concentration, velocity and pressure profile at the full reactor length. The main purpose of steady state model was to study the velocity and concentration profile of the chemical species BA, ECA & ECC involved in the Knoevenagel condensation reaction. The experimental parameters like reaction enthalpy, universal gas constant, different reaction temperatures, rate constants and the input flow rates were measured and were used as input variables for the modeling.

The model was developed at three temperatures of 10°C, 25°C and 40°C. The reactor internal diameter was 4.6 mm and it was 100 mm in length. The basic properties of ethanol as a solvent were taken with the porous material added having the defined permeability and porosity. The molar masses, densities and reaction rate of the reactants BA, ECA and the product ECC along with the other thermodynamic properties were added in the chemistry interface of the model.

3.4.1 Governing Equations

In order to develop a macro meso porous CFD model for a diluted species the following steady state convective-diffusive transport equation was applied to the homogenized porous monolithic reactor:

$$\nabla . J_i + u . \nabla c_i = R_i + S_i \tag{8}$$

13

Whereas:

$$J_i = -(D_{D,i} + D_{e,i})\nabla c_i \tag{9}$$

- "J_i"is the total flux

- "u" the flow velocity within the porous domain calculated by the brinkman's equation

- "c_i" is the species concentration for mass transfer

- "R_i" describe the rate of formation of species ECC as shown in the equation Eq (3)

- $D_{D,i}$ the molecular diffusivity also abbreviated by "D_{AB}" calculated by applying Eq (5)

- $D_{e,i}$ is the effective diffusivity

The following boundary conditions were applied at the inlet and outlet of the monolithic reactor:

Inlet boundary conditions: $c_i = c_{0,i}$

Outer wall conditions: no slip conditions

Outlet boundary conditions: $nD_i\nabla c_i = 0$

The flow in the monolithic reactor takes place inside the macro pores mainly by the process of convection while inside the meso porous structure the flow is due to diffusion. The equations (8) & (9) are the basic mass transport equations that couple the flow transport with the reaction kinetics within the porous monolithic reactor and are applied in the simulation of the reactants BA, ECA and product ECC concentration along the length of the monolithic reactor.

The fluid flow velocity "u" was calculated by applying brinkman equation on the monolithic porous reactor geometry for the steady state conditions as given by the Eq (10):

$$K = \mu \frac{1}{\epsilon_P}\left(\nabla u + (\nabla u^T)\right) - \frac{2}{3}\mu \frac{1}{\epsilon_p}(\nabla . u)I \tag{10}$$

Whereas

- μ (kg m^{-1}s^{-1}) is the dynamic viscosity of the fluid

- u (m s^{-1}) is the velocity vector

- ρ (kg m^{-3}) is the density of the fluid

- p (Pa) is the pressure

- ε_p is the porosity

- κ (m^2) is the permeability of the porous medium, and

- Influence of gravity and the other volume forces can be accounted for via the force term "F" (kg/ (m^2.s^2)

The following boundary conditions were applied in order to solve the Brinkman equation:

Inlet boundary conditions: Fully developed flow

Outer wall boundary: No slip conditions

Outlet boundary conditions: P= 4560000 Pa with suppress backflow

3.5 Pore scale modeling

Pore network modeling is a pore-scale method for studying the transport phenomena and fluid flow in porous media and it accounts for the true geometrical heterogeneity of the porous material at the pore scale. The pore scale modeling provide detailed pore-level information even when the material is highly anisotropic or extremely thin and bulk fluid properties are used in a pore-scale model, which are widely available in the literature. It is a feasible way to perform a pore-scale study on hierarchical porous materials [42].

Pore network modeling is a powerful tool for studying transport in hierarchical materials, most of the available works in this area date back almost two decades, such as the works of Meyers and Liapis. and Petropoulos [47,49,50].

Petropoulos et al. studied the transport in hierarchical materials [50] however, the size of the network they chose, presumably due to the limited processing power, was not large enough to entail the interesting interactions between structural features and transport properties. Moreover, the hierarchical network they proposed included

macro-pores mapped onto nano-pores rather than a true hierarchical network [42]. In addition, the influences of the different structural parameters on transport properties were also not studied. Meyers and Liapis worked further on the framework developed by Petropoulos et al. to incorporate the reactive transport with advection in hierarchical materials in the context of an adsorption column [47,49].

Modeling transport in porous materials is a classic and well-established area of research. Pore scale modeling reduces the higher computational cost that is employed to capture the pore level details. The reason is the shorter mixing time and because of the small length scale of the pores therefore it can be assumed that within an individual pore the variations of the intensive properties such as concentration and pressure is negligible which reduces the cost of computation [42].

The term pore-scale model is used only for those models which solve transport equations simultaneously at all length scales within the porous domain. It is such a modeling framework that includes the structure impact on reactive transport in hierarchically porous materials that would be a strong and powerful tool for optimal design of catalyst supports used for the various applications [51,52].

3.5.1 SEM CFD Modeling

The SEM image of the porous macro meso porous monolith was taken from the Haas et al. The image was reduced to 5 µm by taking a scale of 10500 pixels/ µm; the scaled image was made binary and finally converted into TIFF format using Image J software. The SEM TIFF image was further refined and processed in Inkscape software to finally obtain an SEM COMSOL dxf file. The monolith geometry was imported in the COMSOL Multiphysics and it was enclosed in a square geometry of 5.2 µm. The monolithic skeleton was considered as meso pores and the free flow path taken as the macro pores. The free and porous media flow interface was used to compute the pressure fields and velocity of the fluid of a single phase flow where the free flow is connected to the porous medium. The steady state convective-diffusive transport Equations (8) & (9) were applied in order to develop a macro meso porous SEM CFD model for a diluted species to the porous SEM monolith.

To solve the transport of diluted species in porous media interface for SEM CFD modeling the following boundary conditions were used:

Inlet boundary conditions: $c_i = c_{0,i}$

Outer wall conditions: no slip conditions

Outlet boundary conditions: $nD_i \nabla c_i = 0$

The fluid flow velocity in the SEM Monolithic geometry was calculated by applying brinkman's equation given as follows:

$$\rho \,.\, (u.\nabla).\,u = \nabla.\,[-pI + K] + F \qquad (11)$$

Whereas

- ρ (kg m^{-3}) is the density of the fluid

- u (m s^{-1}) is the velocity vector

- p (Pa) is the pressure

- Influence of gravity and the other volume forces can be accounted for via the force term "F" (kg/ (m^2.s^2)

- κ (m^2) is the permeability of the porous medium, and

The following boundary conditions were applied in order to solve the free and porous media flow:

Inlet boundary conditions: Fully developed flow

Outer wall boundary: No slip conditions

Outlet boundary conditions: P= 4560000 Pa with suppress backflow

3.6 Meshing

In this study coarse physics controlled mesh was applied to the homogenized macro-meso porous monolith model. However at the pore scale SEM modeling finer physics controlled mesh was applied to monolith SEM geometry.

3.7 COMSOL Solvers

The Stationary solver is used in the modeling and simulation of CFD macro meso porous monolithic reactor and SEM CFD modeling. This solver used to find out the solution to the linear and nonlinear stationary problems (steady state problems). This solver was automatically used when a stationary study was added to the monolith model and the stationary study generates equation without any time derivatives.

Chapter 4

Results and Discussion

4.1 Model validation

The 2D axisymmetric steady state homogenized model was developed by considering convection in the macro pores and diffusional transport of diluted species in the meso pores of the hierarchical monolith structure. The model was simulated by commercial CFD software COMSOL MULTIPHYSICS 6.1. Figure 1 compared the experimental conversion results and model simulation results of the Knoevenagel condensation reaction and it showed that the model results well matched with the experimental results of Haas et al. [11] at different temperatures with maximum of 4-7% error which shows the robustness of the model. As seen in the Figure 1 the model results at 10°C very well matched with the experimental results for the corresponding, however a slight deviation of 4-7% between experimental and modelling results can be observed for 25°C and 40°C respectively during the initial phase of the reaction. The simulation results were in good agreement with the experimental results once the reaction reaches steady-state condition for both the cases. These initial reaction times correspond to high flow rate inside the reactor. Based on the model validation, it can be concluded that model well matched with the experimental results and was then applied to obtain some important results which were not possible with the experimental setup like the concentration change along the length of the reactor and thus to optimize the reactor size for the particular reactions.
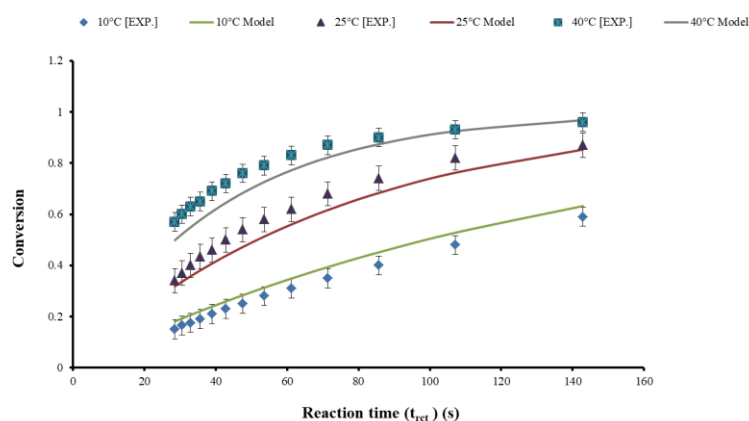

Figure 3: Model validation plot at 10°C (283 K), 25°C (298K) & 40°C (313 K) [11]

Firstly, the velocity profiles were obtained from the modeling results by varying the flow rate from 0.5 mL min^{-1} to 3 mL min^{-1}. These values were chosen based on the experimental data of Haas et al., 2017 [11]. The flow in porous monolith reactors is governed by the equation of continuity and momentum that converges into Brinkman's equation. It is an extension of Darcy's equation that describes slow flow of fluids through porous media [53]. The fluid velocity was calculated by applying brinkman's equation on the macro meso porous reactor and it gives a good explanation of flowing fluids through the monolith reactor [54,55,56,57] . Figure 4(a) (b) (c) (d) shows the contours of velocity profile along the length of the monolith porous reactor with the arrows in the direction of flow. The flow velocity increases with the increase of flow rate at the three temperatures and there was no change in velocity observed with increasing temperature. The simulated fluid flow velocity resulted to be 2.0058e-4 m s^{-1} at 0.2 ml min^{-1} and it increased to 0.003 m sec^{-1} at 3 ml min^{-1}. The relationship between flow rate and pressure drop is of significant importance through the continuous flow monolith reactor because it provides additional information that is helpful in the assessment of process economics [58] and in our study a linear increase in the pressure drop is observed with the fluid flow velocity.
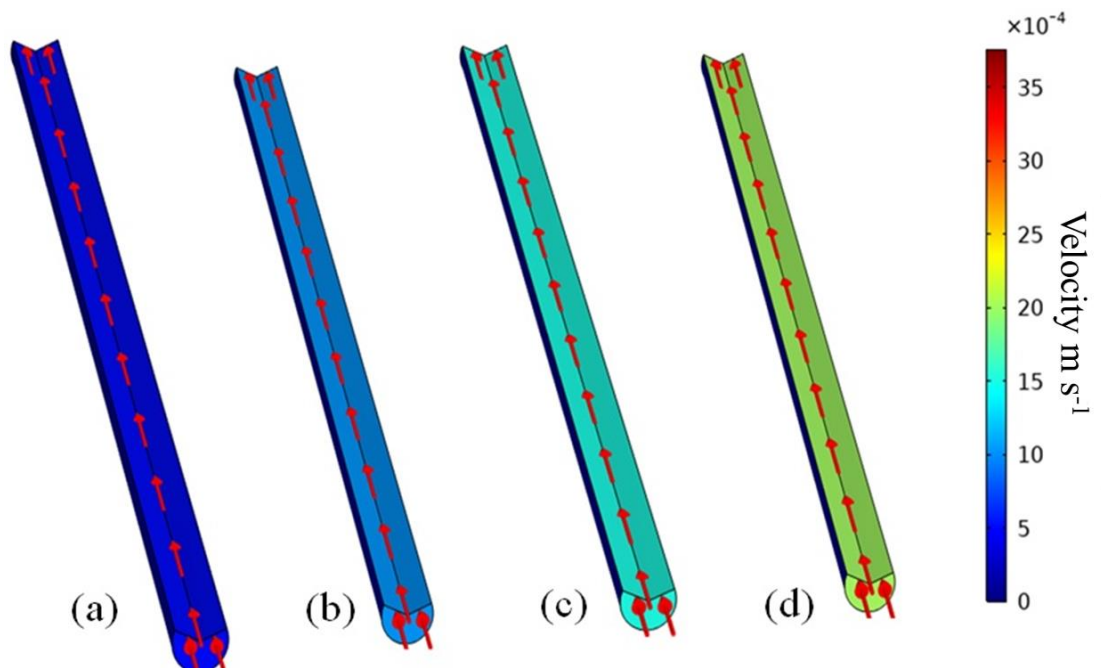

Figure 4: Velocity profile along the length of the reactor at (a) Q=0.5 ml min^{-1} (b) Q=1 ml min^{-1} (c) Q= 2 ml min^{-1} (d) Q=3 ml min^{-1} at all the three temperatures

4.2 Concentration profile

4.2.1 Reactant ECA Concentration

Table 2 shows the change in ECA Concentration with the increase in flow rate. There are two important outcomes from the concentration profile of ECA. The first is the increase in the final ECA Concentration with the increase in flow rate at the three selected temperatures. The second is the decrease in the final concentration values as the temperature increases from 10°C (283K) to 25°C (298K) and finally to 40°C (313K) at any specific flow rate. Figure 5, 7 & 9 shows the contours of decrease in final ECA concentration along the length of the monolith porous reactor at 1 ml/min temperatures of 10°C (283K), 25°C (298K) & 40°C (313K) respectively

Q (ml/min)	FINAL ECA Concentration (mol/m^3) 10°C (283K)	FINAL ECA Concentration (mol/m^3) 25°C (298K)	FINAL ECA Concentration (mol/m^3) 40°C (313K)
0.2	1.2428	0.079527	7.99E-04
0.4	5.5714	1.4085	0.14104
0.6	9.1893	3.6739	0.79211
0.8	11.802	5.9335	1.8771
1	13.713	7.9112	3.1502
1.2	15.157	9.5834	4.4491
1.4	16.28	10.99	5.6932
1.6	17.177	12.179	6.8497
1.8	17.908	13.193	7.9094
2	18.516	14.063	8.8741
2.2	19.028	14.818	9.7501
2.4	19.466	15.478	10.546
2.6	19.844	16.06	11.27
2.8	20.174	16.576	11.93
3.0	20.465	17.036	12.533

Table 2: Final reactant ECA Concentration at different flow rates in a porous monolithic reactor at (a) 10°C (283K) (b) 25°C (298K) (c) 40°C (313K)

4.3 Conversion

According to the Haas et al. [11] the initial concentration of the reactant ECA was 25mol/m^3. The final ECA concentration simulated results show a decrease in the concentration thus converting into the product ECC. Case 1, 2 & 3 shows the initial and the simulated final ECA concentration values at selected temperatures and the final conversion calculated from the equation 13 taken from the Haas et al [11] that is as follows:

$$conversion = final\ product\ ECC\ Concentration/Initial\ ECA\ Concentration \quad (12)$$

$$conversion = (initial - final)ECA\ Concentration/Initial\ ECA\ Concentration \quad (13)$$

4.3.1   CASE 1: AT TEMP 10°C (283K)

Q (ml/min)	Initial ECA Concentration (mol/m^3)	Final ECA Concentration (mol/m3)	Conversion	% Conversion
0.2	25	1.2428	0.950288	95.0288
0.4	25	5.5714	0.777144	77.7144
0.6	25	9.1893	0.632428	63.2428
0.8	25	11.802	0.52792	52.792
1	25	13.713	0.45148	45.148
1.2	25	15.157	0.39372	39.372
1.4	25	16.28	0.3488	34.88
1.6	25	17.177	0.31292	31.292
1.8	25	17.908	0.28368	28.368
2	25	18.516	0.25936	25.936
2.2	25	19.028	0.23888	23.888
2.4	25	19.466	0.22136	22.136
2.6	25	19.844	0.20624	20.624
2.8	25	20.174	0.19304	19.304
3.0	25	20.465	0.1814	18.14

Table 3: Conversion on the basis of reactant ECA into product ECC at 10°C (283K)
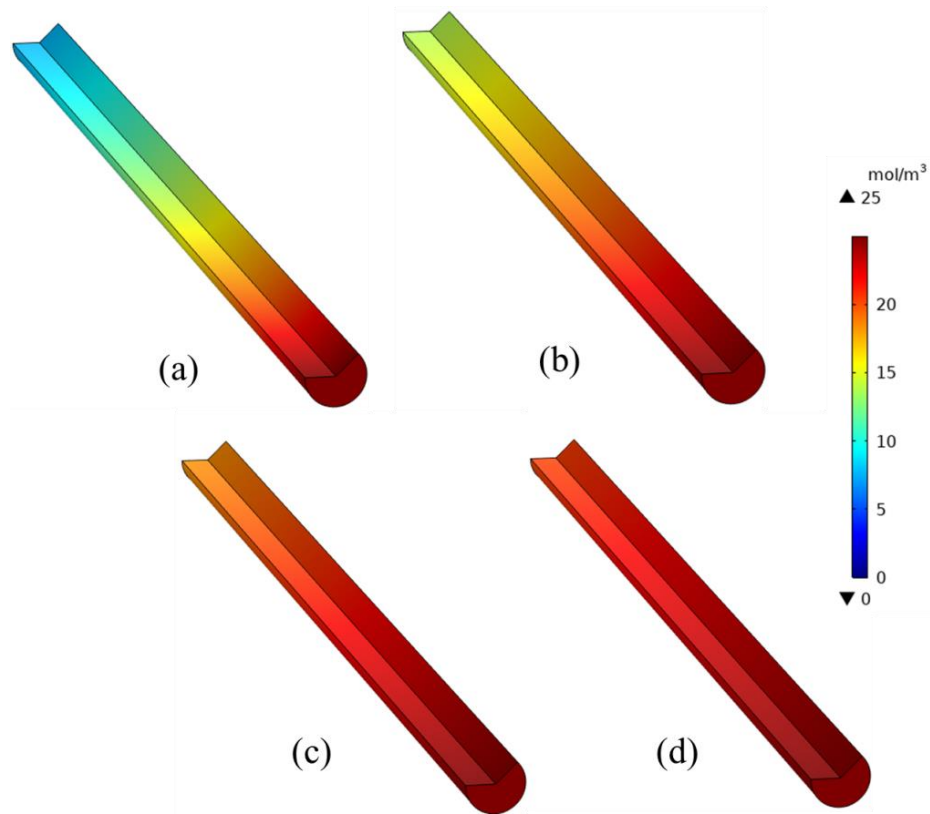
Figure 5: ECA Concentration profile along the length of the reactor at temperature 10°C (283 K) at (a) Q=0.5 ml min^{-1} (b) Q=1 ml min^{-1} (c) Q= 2 ml min^{-1} (d) Q=3 ml min^{-1}
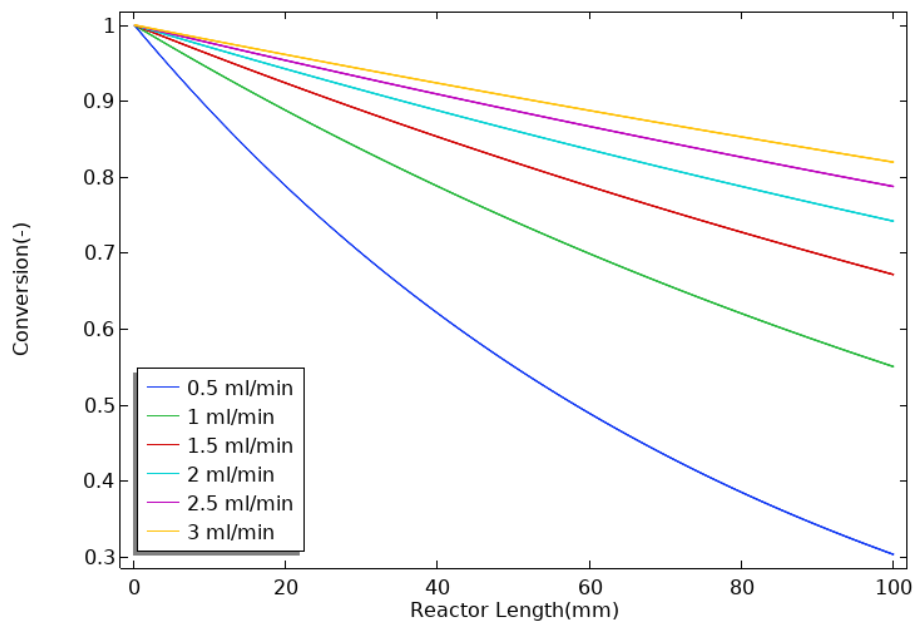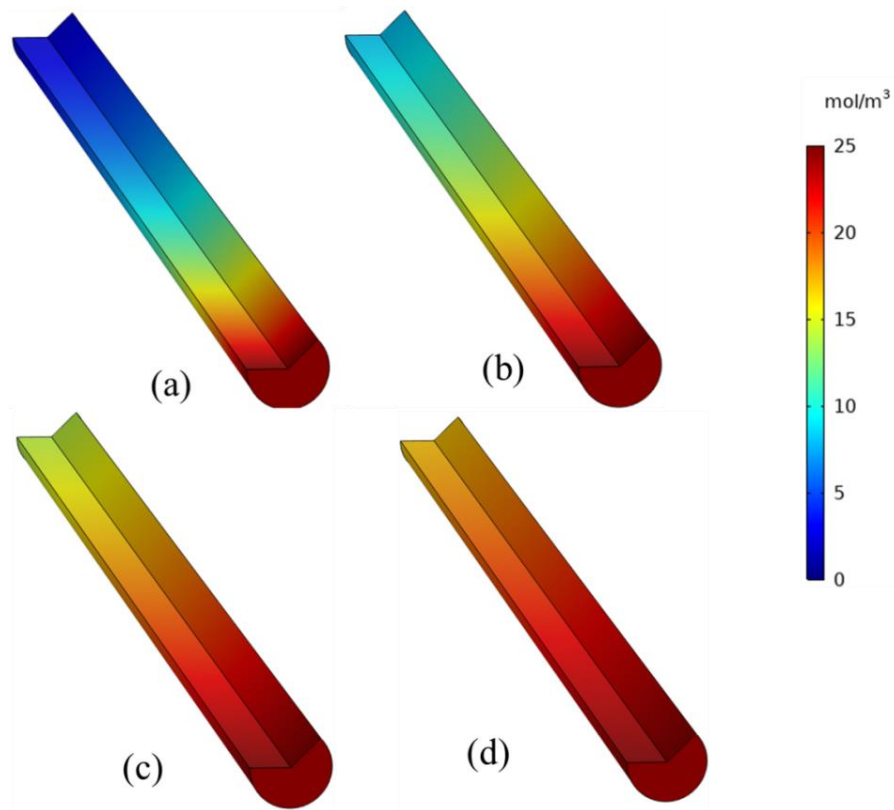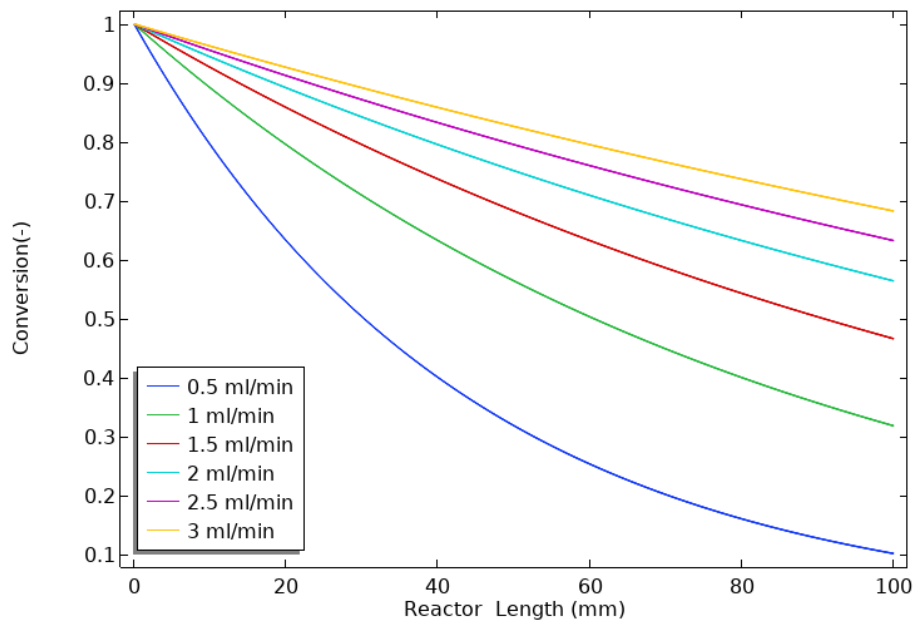

Figure 6 : ECA Conversion along the length of the reactor at temperature 10°C (283 K) (a) Q=0.5 ml min^{-1} (b) Q=1 ml min^{-1} (c) Q= 1.5 ml min^{-1} (d) Q=2 ml min^{-1} (e) Q=2.5 ml min^{-1} (f) Q=3 ml min^{-1}

4.3.2 CASE 2: AT TEMP 25°C (298K)

Q (ml/min)	Initial ECA Concentration (mol/m³)	Final ECA Concentration (mol/m3)	Conversion	% Conversion
0.2	25	0.079527	0.996819	99.68189
0.4	25	1.4085	0.94366	94.366
0.6	25	3.6739	0.853044	85.3044
0.8	25	5.9335	0.76266	76.266
1	25	7.9112	0.683552	68.3552
1.2	25	9.5834	0.616664	61.6664
1.4	25	10.99	0.5604	56.04
1.6	25	12.179	0.51284	51.284
1.8	25	13.193	0.47228	47.228
2	25	14.063	0.43748	43.748
2.2	25	14.818	0.40728	40.728
2.4	25	15.478	0.38088	38.088
2.6	25	16.06	0.3576	35.76
2.8	25	16.576	0.33696	33.696
3.0	25	17.036	0.31856	31.856

Table 4: Conversion on the basis of reactant ECA into product ECC at 25°C (298K) at flow rate 0.2-3 ml/min

Figure 7: ECA Concentration profile along the length of the reactor at temperature 25°C (298 K) at (a) Q=0.5 ml min^{-1} (b) Q=1 ml min^{-1} (c) Q= 2 ml min^{-1} (d) Q=3 ml min^{-1}
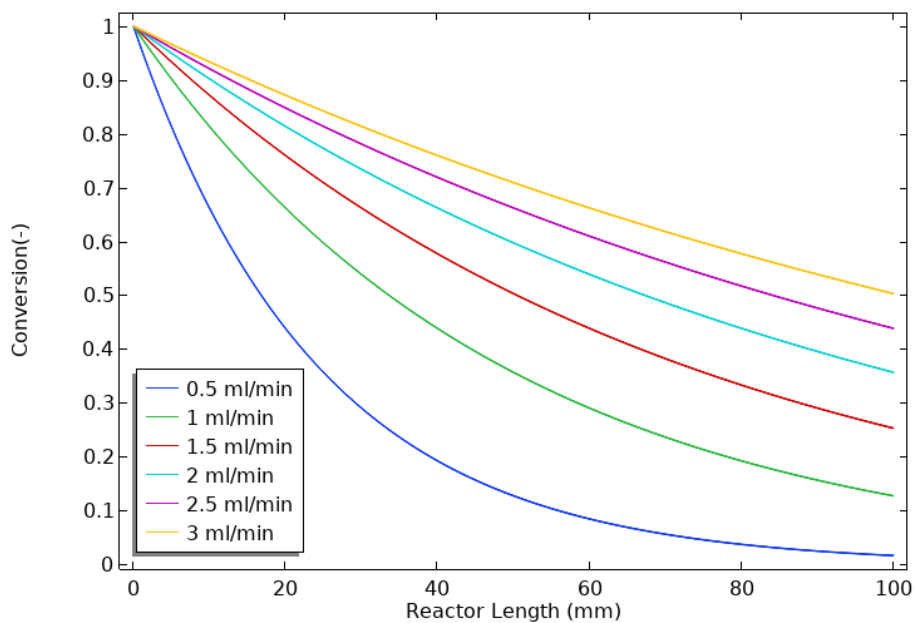

Figure 8 : ECA Conversion along the length of the reactor at temperature 25°C (298 K) (a) Q=0.5 ml min^{-1} (b) Q=1 ml min^{-1} (c) Q= 1.5 ml min^{-1} (d) Q=2 ml min^{-1} (e) Q=2.5 ml min^{-1} (f) Q=3 ml min^{-1}

4.3.3 CASE 3: AT TEMP 40°C (313K)

Q (ml/min)	Initial ECA Concentration (mol/m³)	Final ECA Concentration (mol/m³)	Conversion	%Conversion
0.2	25	7.99E-04	0.999968	99.9968
0.4	25	0.14104	0.994358	99.43584
0.6	25	0.79211	0.968316	96.83156
0.8	25	1.8771	0.924916	92.4916
1	25	3.1502	0.873992	87.3992
1.2	25	4.4491	0.822036	82.2036
1.4	25	5.6932	0.772272	77.2272
1.6	25	6.8497	0.726012	72.6012
1.8	25	7.9094	0.683624	68.3624
2	25	8.8741	0.645036	64.5036
2.2	25	9.7501	0.609996	60.9996
2.4	25	10.546	0.57816	57.816
2.6	25	11.27	0.5492	54.92
2.8	25	11.93	0.5228	52.28
3.0	25	12.533	0.49868	49.868

Table 5: Conversion on the basis of reactant ECA into product ECC at 40°C (313K)
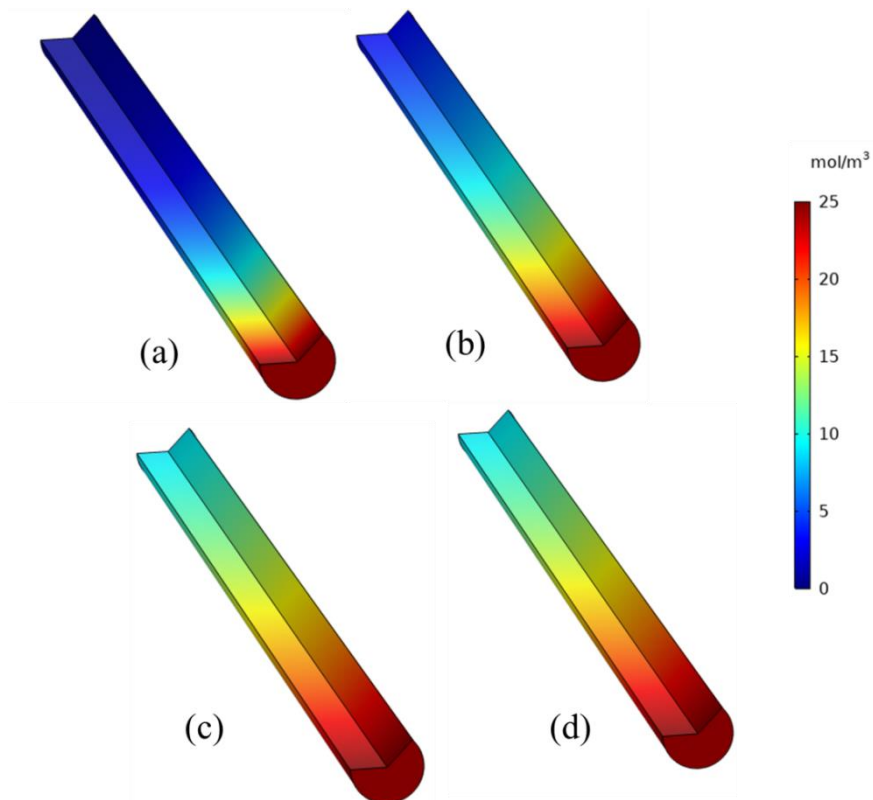
Figure 9: ECA Concentration profile along the length of the reactor at temperature 40°C
(313 K) at (a) Q=0.5 ml min⁻¹ (b) Q=1 ml min⁻¹ (c) Q= 2 ml min⁻¹ (d) Q=3 ml min⁻¹

Figure 10: ECA Conversion along the length of the reactor at temperature 40 °C (313 K) (a)
Q=0.5 ml min⁻¹ (b) Q=1 ml min⁻¹ (c) Q= 1.5 ml min⁻¹ (d) Q=2 ml min⁻¹ (e) Q=2.5 ml min⁻¹
(f) Q=3 ml min⁻¹

4.4 Effect of structural parameters on conversion

Once the model was validated, the effect of different parameters was studied. The following figures shows the plot in which the meso porosity of monolith is the key parameter. The increase in meso porosity enhances the surface area providing more active sites for the reaction kinetics thus finally resulting into increased overall conversion. The following are the cases based on different conversion results at different meso porosity values for the three reaction temperatures.

(i)   Case 1: Q= 0.5 ml min^{-1}
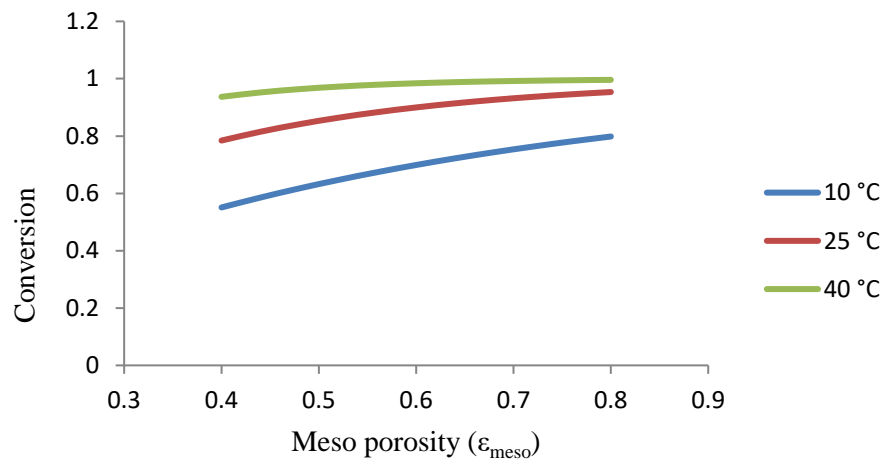
Figure 11 : Effect of meso porosity on conversion at temperature (a) 10 °C (283 K) (b)25 °C (298 K) (c) 40 °C (313 K) at a flow rate of 0.5 ml min^{-1}

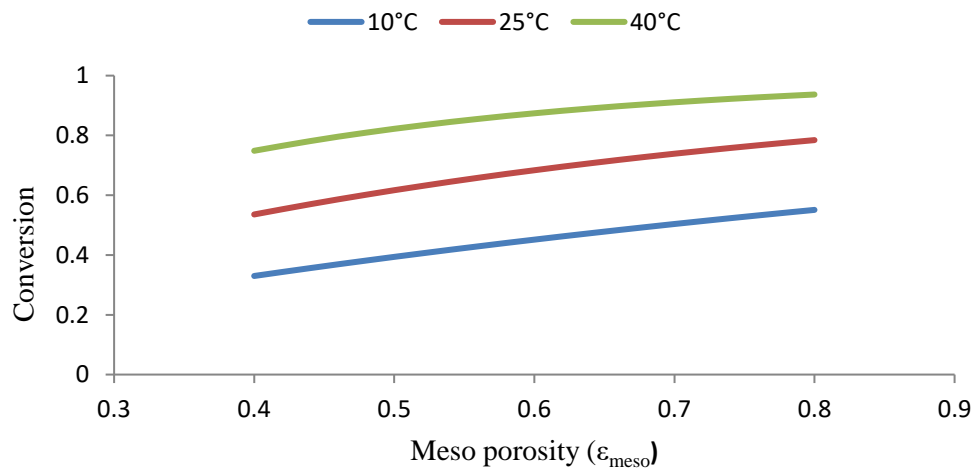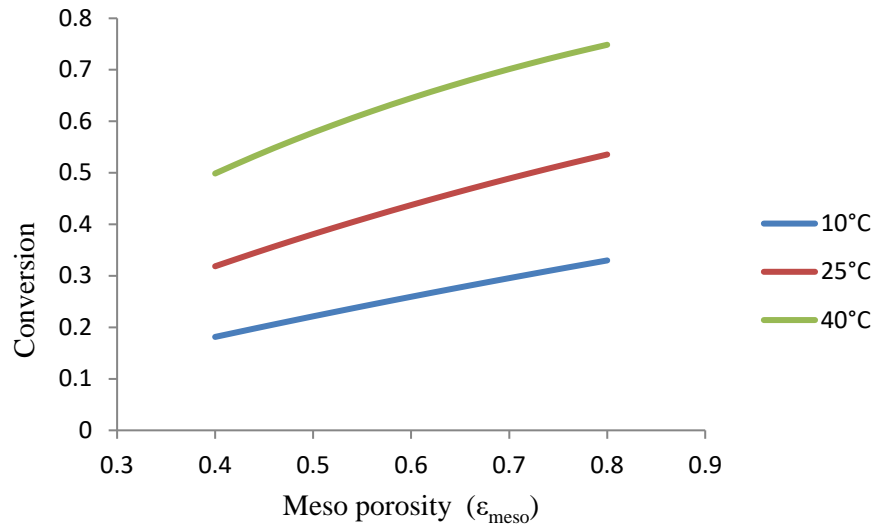**(ii)   Case 2: Q= 1 ml min^{-1}**

Figure 12 : Effect of meso porosity on conversion at temperature (a) 10 °C (283 K) (b)25 °C (298 K) (c) 40 °C (313 K) at a flow rate of 1 ml min^{-1}

(iii)   Case 3: Q= 2 ml min^{-1}

Figure 13 : Effect of meso porosity on conversion at temperature (a) 25 °C (283 K) (b)25 °C
(298 K) (c) 40 °C (313 K) at a flow rate of 2 ml min^{-1}
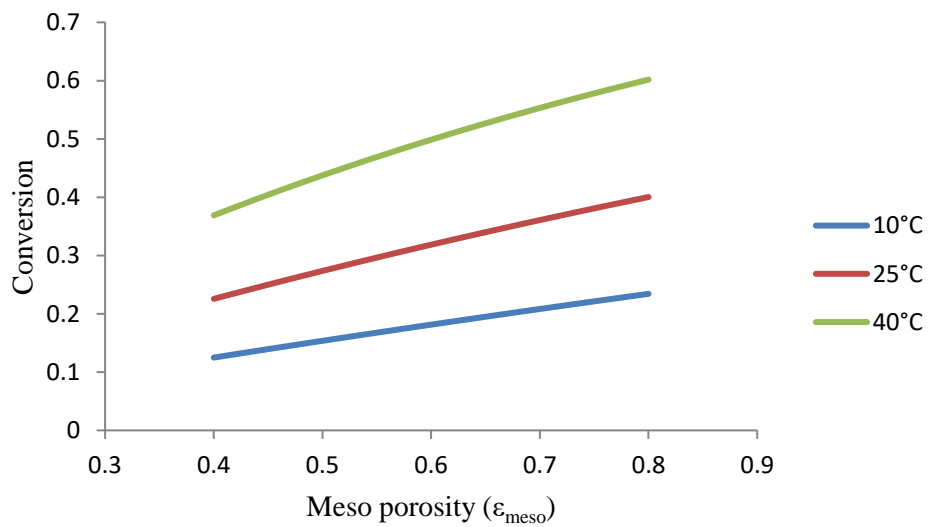
(iv)   Case 4: Q= 3 ml min^{-1}

Figure 14 : Effect of meso porosity on conversion at temperature (a) 25 °C (283 K) (b)25 °C
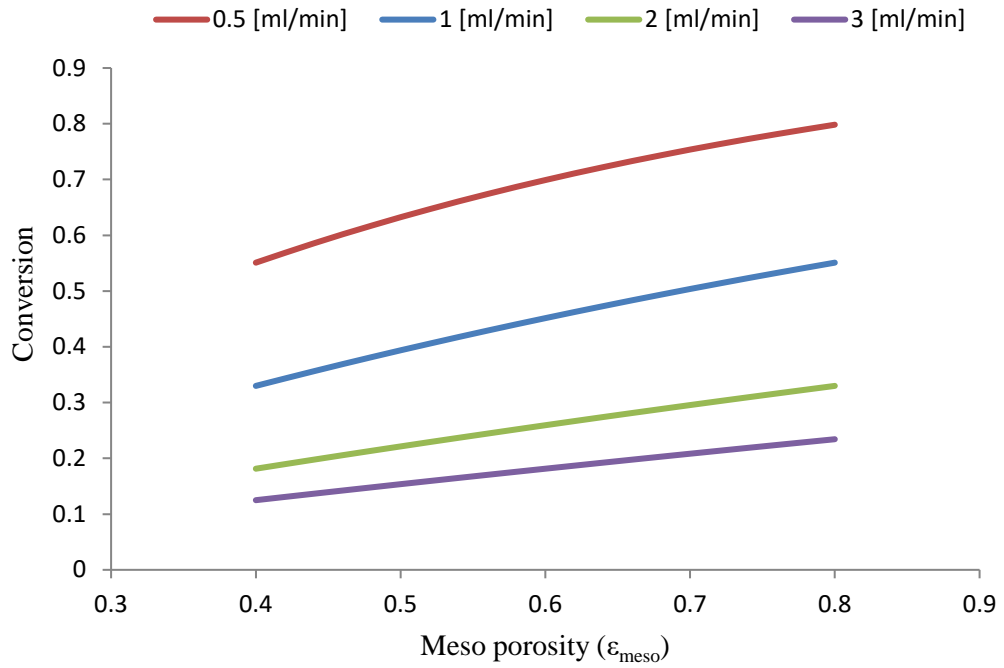(298 K) (c) 40 °C (313 K) at a flow rate of 3 ml min^{-1}

Figure 15: Effect of meso porosity on conversion at temperature 10 °C (283 K) at (a) Q=0.5 ml min^{-1} (b) Q=1 ml min^{-1} (c) Q=2 ml min^{-1} (d) Q=3 ml min^{-1}
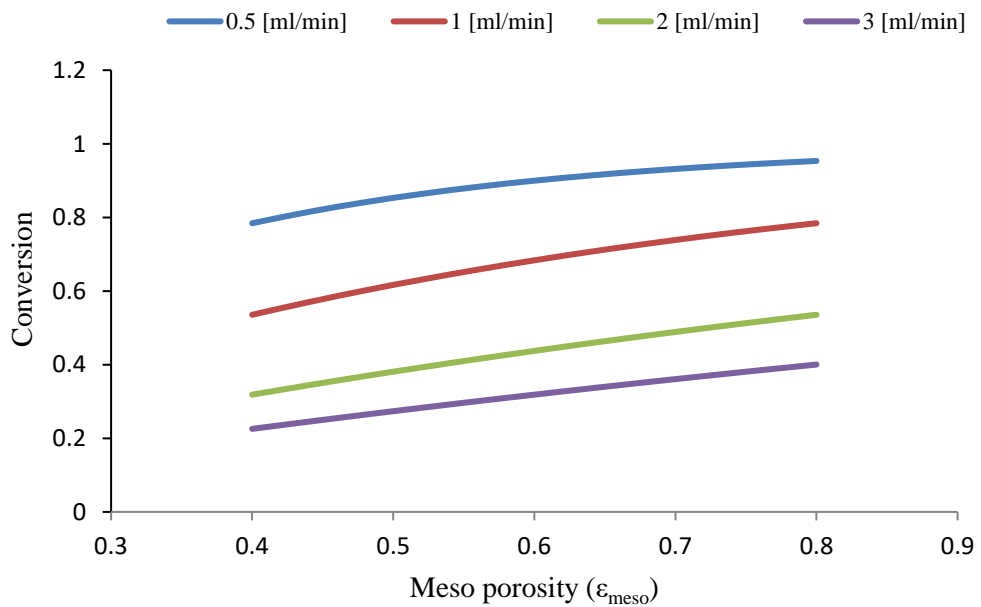

Figure 16 : Effect of meso porosity on conversion at temperature 25 °C (298 K) at (a) Q=0.5 ml min^{-1} (b) Q=1 ml min^{-1} (c) Q=2 ml min^{-1} (d) Q=3 ml min^{-1}
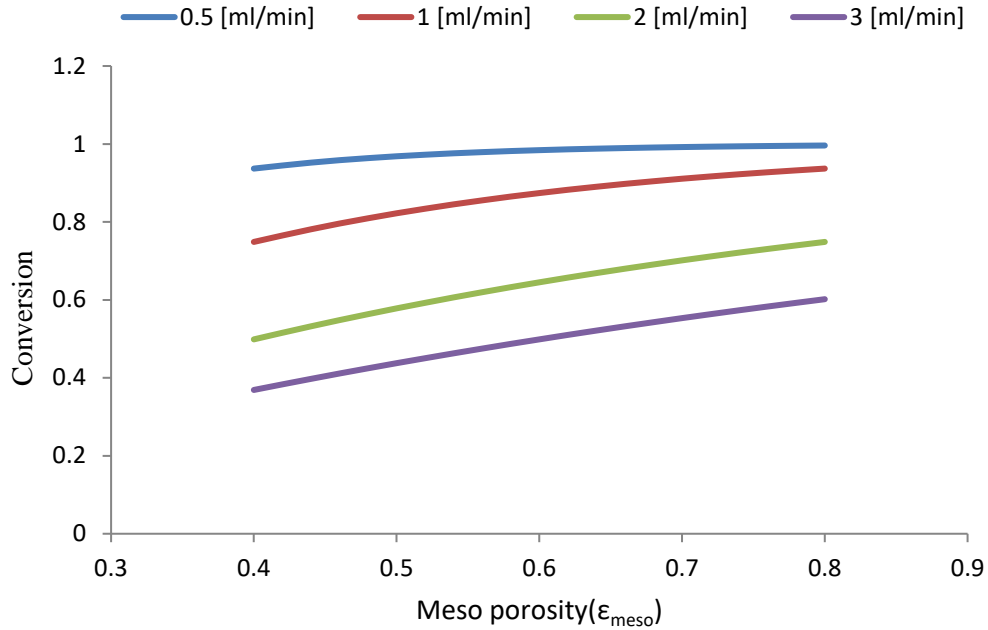
Figure 17 : Effect of meso porosity on conversion at temperature 40 °C (313 K) at (a) Q=0.5 ml min^{-1} (b) Q=1 ml min^{-1} (c) Q=2 ml min^{-1} (d) 3 ml min^{-1}

It is seen from the meso porosity versus conversion plots that the conversion is more at lowest flow rate of 0.5 ml/min for all temperatures because of the increased residence time for the reactant ECA converted into product ECC. It is also observed that with the increase of temperature coversion is increased at all flow rates.

4.5   SEM CFD MODELING

The scanning electron microscopy (SEM) image of macro meso porous monoliths was used to observe the transport phenomenon and reaction kinetics at the pore scale level. Most important of all is that we have taken the   actual SEM data and performed pore scale SEM CFD modeling by coupling flow with transport phenomenon.

The free and porous media flow and transport of diluted species along with the boundary conditions were applied to calculate the velocity and to observe the change in concentration through the monolith structure at the nano scale. Figure 8(a) shows the velocity contours of the flowing reacting species through the monolith. Figure 8 (b) & 8 (c) shows the change in the concentration of reactant ECA and product ECC through the monolithic structure.

There are two regions in the pore scale SEM CFD modeling; one is free flow path that are the macro pores responsible for the flow of reacting species to the active sites and product transport from the active sites to the main bulk of fluid. Another one that
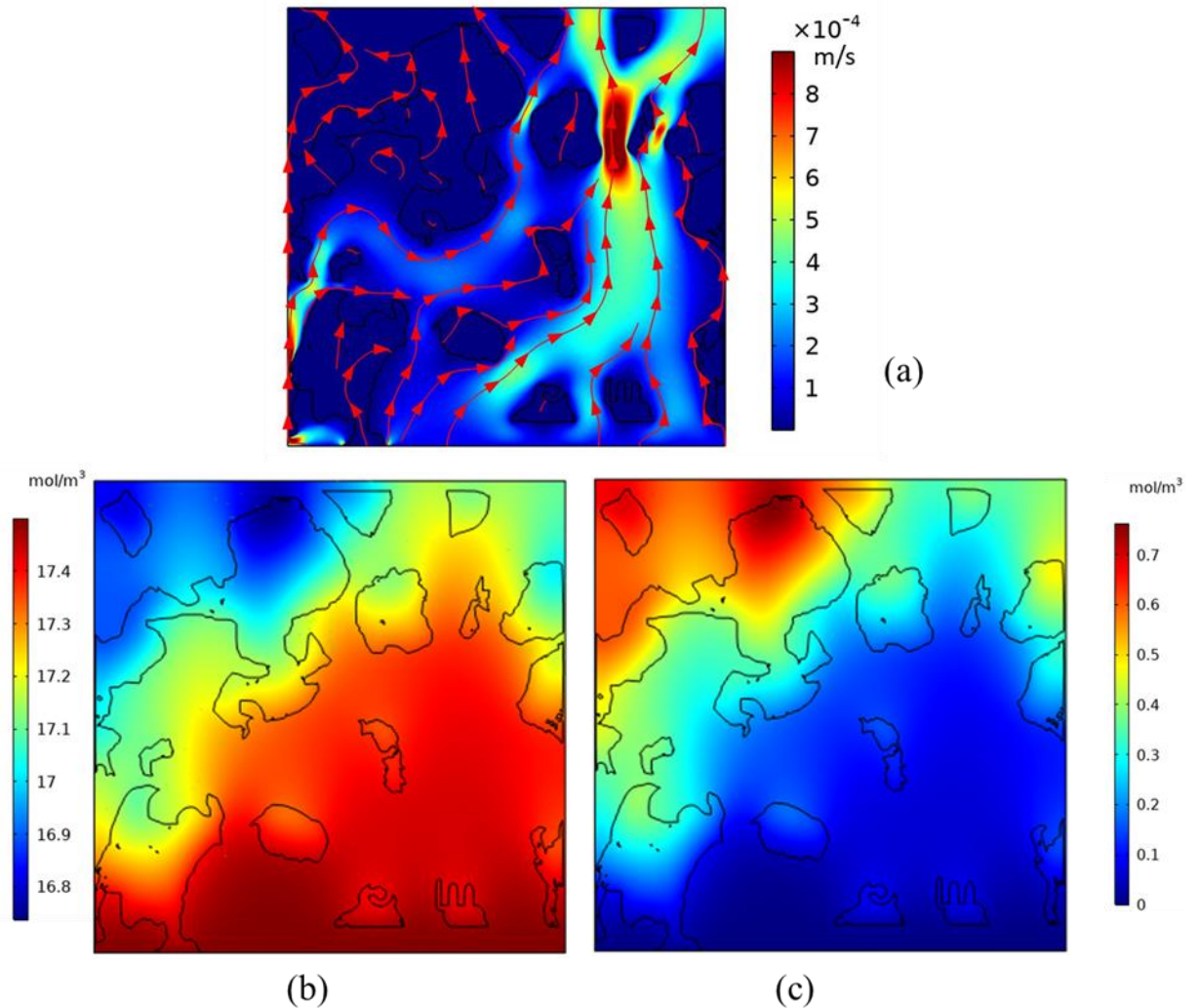

Figure 18: (a) Velocity flow through the monolith structure (b) Concentration contour of reactant ECA (c) Concentration contour of product ECC

is seen in the figure 18 are the spots on the SEM CFD contours that are actually the meso pores in the monolith skeleton where all the reaction kinetics takes place in the presence of immobilized catalyst. The colour gradients in the figure 8 (b) & 8 (c) are a proof that reaction kinetics is taking place in the macro meso porous monolith converting the reactents into products. The velocity profile, concentraton contours and the conversion results proved monoliths to be an effective and efficient catalyst supports for faster reaction kinetics and better transport mechanism.

Conclusions

In this study, a CFD homogenized model of macro meso porous monolith is developed for the Knoevenagel condensation of Benzaldehyde and Ethyl cyanoacetate with Ethanol as a solvent to produce Ethyl trans-α-cyanocinnamate. The modeling involves the use of Brinkmans equation for calculation of fluid flow velocity and also the application of convective-diffusive mass transport equations. The model is validated against the experimental data and it provide deep insights into the transport phenomenon and reaction kinetics. The reaction rate is temperature dependent so the conversion is highest as the temperature is maximum. This present study also take into consideration the effect of structural parameters of the monolith on the overall reaction conversion. Meso porosity of monolith is an important structural parameter that is pivotal for better reaction conversion. The increase in the meso porosity values provide more active sites for reaction kinetics thus increasing the surface area. Hence the increase in meso porosity with varying flowrate or temperatures enhances the conversion of the Knoevenagel condensation rection.

This is the first research work to perform SEM CFD modeling from actual SEM data by coupling flow with the transport phenomenon. The simulation results show a complete description of the fluid flow in the macro pores with little conversion and reaction kinetics with maximum conversion in the meso pores of the monolith structure. The findings of this study can be used to apply for further modeling for any other reaction kinetics and also employing macro meso porous monoliths on a large scale. The future prospects can include further optimizing the structural parameters to increase reaction conversion and productivity.

Reference

[1]   B. W. J. Chen, L. Xu, and M. Mavrikakis, "Computational Methods in Heterogeneous Catalysis," *Chem. Rev.*, vol. 121, no. 2, pp. 1007–1048, Jan. 2021, doi: 10.1021/acs.chemrev.0c01060.

[2]   N. Linares, S. Hartmann, A. Galarneau, and P. Barbaro, "Continuous Partial Hydrogenation Reactions by Pd@unconventional Bimodal Porous Titania Monolith Catalysts," *ACS Catal.*, vol. 2, no. 10, pp. 2194–2198, Oct. 2012, doi: 10.1021/cs3005902.

[3]   A. Dhakshinamoorthy, S. Navalon, A. M. Asiri, and H. Garcia, "Metal organic frameworks as solid catalysts for liquid-phase continuous flow reactions," *Chem. Commun.*, vol. 56, no. 1, pp. 26–45, 2020, doi: 10.1039/C9CC07953J.

[4]   C. G. Frost and L. Mutton, "Heterogeneous catalytic synthesis using microreactor technology," *Green Chem.*, vol. 12, no. 10, p. 1687, 2010, doi: 10.1039/c0gc00133c.

[5]   D. K. Dumbre, T. Mozammel, Pr. Selvakannan, S. B. A. Hamid, V. R. Choudhary, and S. K. Bhargava, "Thermally decomposed mesoporous Nickel Iron hydrotalcite: An active solid-base catalyst for solvent-free Knoevenagel condensation," *J. Colloid Interface Sci.*, vol. 441, pp. 52–58, Mar. 2015, doi: 10.1016/j.jcis.2014.11.018.

[6]   D. Elhamifar, S. Kazempoor, and B. Karimi, "Amine-functionalized ionic liquid-based mesoporous organosilica as a highly efficient nanocatalyst for the Knoevenagel condensation," *Catal. Sci. Technol.*, vol. 6, no. 12, pp. 4318–4326, 2016, doi: 10.1039/C5CY01666E.

[7]   K. M. Parida and D. Rath, "Amine functionalized MCM-41: An active and reusable catalyst for Knoevenagel condensation reaction," *J. Mol. Catal. Chem.*, vol. 310, no. 1–2, pp. 93–100, Sep. 2009, doi: 10.1016/j.molcata.2009.06.001.

[8]   G. B. B. Varadwaj, S. Rana, and K. M. Parida, "Amine functionalized K10 montmorillonite: a solid acid–base catalyst for the Knoevenagel condensation reaction," *Dalton Trans.*, vol. 42, no. 14, p. 5122, 2013, doi: 10.1039/c3dt32495h.

[9] J. N. Appaturi *et al.*, "A review of the recent progress on heterogeneous catalysts for Knoevenagel condensation," *Dalton Trans.*, vol. 50, no. 13, pp. 4445–4469, 2021, doi: 10.1039/D1DT00456E.

[10] U. Tallarek, F. C. Leinweber, and A. Seidel-Morgenstern, "Fluid Dynamics in Monolithic Adsorbents: Phenomenological Approach to Equivalent Particle Dimensions," *Chem. Eng. Technol.*, vol. 25, no. 12, pp. 1177–1181, Dec. 2002, doi: 10.1002/1521-4125(20021210)25:12<1177::AID-CEAT1177>3.0.CO;2-V.

[11] C. P. Haas, T. Müllner, R. Kohns, D. Enke, and U. Tallarek, "High-performance monoliths in heterogeneous catalysis with single-phase liquid flow," *React. Chem. Eng.*, vol. 2, no. 4, pp. 498–511, 2017, doi: 10.1039/C7RE00042A.

[12] A. Tanimu, S. Jaenicke, and K. Alhooshani, "Heterogeneous catalysis in continuous flow microreactors: A review of methods and applications," *Chem. Eng. J.*, vol. 327, pp. 792–821, Nov. 2017, doi: 10.1016/j.cej.2017.06.161.

[13] T. A. Nijhuis, A. E. W. Beers, T. Vergunst, I. Hoek, F. Kapteijn, and J. A. Moulijn, "Preparation of monolithic catalysts," *Catal. Rev.*, vol. 43, no. 4, pp. 345–380, Nov. 2001, doi: 10.1081/CR-120001807.

[14] V. Tomašić and F. Jović, "State-of-the-art in the monolithic catalysts/reactors," *Appl. Catal. Gen.*, vol. 311, pp. 112–121, Sep. 2006, doi: 10.1016/j.apcata.2006.06.013.

[15] A. Sachse, A. Galarneau, and B. Coq, "Monolithic flow microreactors improve fine chemicals synthesis," 2011.

[16] H.-L. Liao *et al.*, "Preparation of Pd/γ-Al2O3/nickel foam monolithic catalyst and its performance for selective hydrogenation in a rotating packed bed reactor," *Chin. J. Chem. Eng.*, vol. 41, pp. 311–319, Jan. 2022, doi: 10.1016/j.cjche.2021.08.026.

[17] A. Galarneau *et al.*, "Hierarchical porous silica monoliths: A novel class of microreactors for process intensification in catalysis and adsorption," *Comptes Rendus Chim.*, vol. 19, no. 1–2, pp. 231–247, Jan. 2016, doi: 10.1016/j.crci.2015.05.017.

[18] M. Griebel, S. Knapek, and G. W. Zumbusch, *Numerical simulation in molecular dynamics: numerics, algorithms, parallelization, applications*. in Texts in computational science and engineering, no. 5. Berlin: Springer, 2007.

[19] I. Battiato, D. M. Tartakovsky, A. M. Tartakovsky, and T. Scheibe, "On breakdown of macroscopic models of mixing-controlled heterogeneous reactions in porous media," *Adv. Water Resour.*, vol. 32, no. 11, pp. 1664–1673, Nov. 2009, doi: 10.1016/j.advwatres.2009.08.008.

[20] S. Whitaker, "Theory and applications of transport in porous media: The method of volume averaging," *Neth. Kluwer Acad. Publ.*, p. 81, 1999.

[21] W. G. Gray and C. T. Miller, *Introduction to the thermodynamically constrained averaging theory for porous medium systems*, vol. 696. Springer, 2014.

[22] R. Acharya, S. Van der Zee, and A. Leijnse, "Transport modeling of nonlinearly adsorbing solutes in physically heterogeneous pore networks," *Water Resour. Res.*, vol. 41, no. 2, 2005.

[23] G. Papanicolau, A. Bensoussan, and J.-L. Lions, *Asymptotic analysis for periodic structures*. Elsevier, 1978.

[24] J. Rubinstein and R. Mauri, "Dispersion and convection in periodic porous media," *SIAM J. Appl. Math.*, vol. 46, no. 6, pp. 1018–1023, 1986.

[25] J. Bear, *Modeling phenomena of flow and transport in porous media*, vol. 1. Springer, 2018.

[26] E. Miroshnikova, "Some new results in homogenization of flow in porous media with mixed boundary condition," Licentiate thesis, comprehensive summary, Luleå tekniska universitet, 2016. Accessed: Sep. 30, 2016. [Online]. Available: http://urn.kb.se/resolve?urn=urn:nbn:se:ltu:diva-26737

[27] I. Battiato *et al.*, "Theory and Applications of Macroscale Models in Porous Media," *Transp. Porous Media*, vol. 130, no. 1, pp. 5–76, Oct. 2019, doi: 10.1007/s11242-019-01282-2.

[28] O. A. Luévano-Rivas, J. J. Quiroz-Ramirez, V. A. Suarez-Toriello, B. Huerta-Rosas, E. Sánchez-Ramirez, and J. G. Segovia-Hernández, "Upscaling of mass and heat transport applied to reactive packing catalytic porous media," *Chem. Eng. Sci.*, vol. 265, p. 118206, Jan. 2023, doi: 10.1016/j.ces.2022.118206.

[29] J. Tu, G. H. Yeoh, C. Liu, and Y. Tao, *Computational fluid dynamics: a practical approach*. Elsevier, 2023.

[30] M. E. Potter, L.-M. Armstrong, and R. Raja, "Combining catalysis and computational fluid dynamics towards improved process design for ethanol

dehydration," *Catal. Sci. Technol.*, vol. 8, no. 23, pp. 6163–6172, 2018, doi: 10.1039/C8CY01564C.

[31] H. Wang *et al.*, "Recent advances in computational fluid dynamics simulation of flotation: a review," *Asia-Pac. J. Chem. Eng.*, vol. 16, no. 5, Sep. 2021, doi: 10.1002/apj.2704.

[32] I. Fechete, Y. Wang, and J. C. Védrine, "The past, present and future of heterogeneous catalysis," *Catal. Today*, vol. 189, no. 1, pp. 2–27, 2012.

[33] G. Somorjai and R. Rioux, "High technology catalysts towards 100% selectivity: Fabrication, characterization and reaction studies," *Catal. Today*, vol. 100, no. 3–4, pp. 201–215, 2005.

[34] A. Corma, "From Microporous to Mesoporous Molecular Sieve Materials and Their Use in Catalysis," *Chem. Rev.*, vol. 97, no. 6, pp. 2373–2420, Oct. 1997, doi: 10.1021/cr960406n.

[35] J. S. Schulze, R. D. Brand, J. G. C. Hering, L. M. Riegger, P. R. Schreiner, and B. M. Smarsly, "DMAP Immobilized on Porous Silica Particles and Monoliths for the Esterification of Phenylethanol in Continuous Flow," *ChemCatChem*, vol. 14, no. 8, Apr. 2022, doi: 10.1002/cctc.202101845.

[36] A. Sachse, A. Galarneau, B. Coq, and F. Fajula, "Monolithic flow microreactors improve fine chemicals synthesis," *New J. Chem.*, vol. 35, no. 2, p. 259, 2011, doi: 10.1039/c0nj00965b.

[37] K. Turke, R. Meinusch, and P. Cop, "Amine-Functionalized Nanoporous Silica Monoliths for Heterogeneous Catalysis of the Knoevenagel Condensation in Flow," *ACS Omega*, 2021.

[38] Y. Xiao, M. Zheng, Z. Liu, J. Shi, F. Huang, and X. Luo, "Constructing a Continuous Flow Bioreactor Based on a Hierarchically Porous Cellulose Monolith for Ultrafast and Nonstop Enzymatic Esterification/Transesterification," *ACS Sustain. Chem. Eng.*, vol. 7, no. 2, pp. 2056–2063, Jan. 2019, doi: 10.1021/acssuschemeng.8b04471.

[39] C. A. Kavale, N. S. Kaisare, and H. Goyal, "Porous Medium Modeling of Catalytic Monoliths Using Volume Averaging," *Ind. Eng. Chem. Res.*, p. acs.iecr.3c00228, May 2023, doi: 10.1021/acs.iecr.3c00228.

[40] A. G. Dixon, "Local transport and reaction rates in a fixed bed reactor tube: Endothermic steam methane reforming," *Chem. Eng. Sci.*, vol. 168, pp. 156–177, Aug. 2017, doi: 10.1016/j.ces.2017.04.039.

[41] J. Petera, L. Nowicki, and S. Ledakowicz, "New numerical algorithm for solving multidimensional heterogeneous model of the fixed bed reactor," *Chem. Eng. J.*, vol. 214, pp. 237–246, Jan. 2013, doi: 10.1016/j.cej.2012.10.020.

[42] M. A. Sadeghi, M. Aghighi, J. Barralet, and J. T. Gostick, "Pore network modeling of reaction-diffusion in hierarchical porous particles: The effects of microstructure," *Chem. Eng. J.*, vol. 330, pp. 1002–1011, Dec. 2017, doi: 10.1016/j.cej.2017.07.139.

[43] J. H. Ghouse and T. A. Adams, "A multi-scale dynamic two-dimensional heterogeneous model for catalytic steam methane reforming reactors," *Int. J. Hydrog. Energy*, vol. 38, no. 24, pp. 9984–9999, Aug. 2013, doi: 10.1016/j.ijhydene.2013.05.170.

[44] H. Bai, J. Theuerkauf, P. A. Gillis, and P. M. Witt, "A coupled DEM and CFD simulation of flow field and pressure drop in fixed bed reactor with randomly packed catalyst particles," *Ind. Eng. Chem. Res.*, vol. 48, no. 8, pp. 4060–4074, 2009.

[45] A. G. Dixon and M. Nijemeisland, "CFD as a design tool for fixed-bed reactors," *Ind. Eng. Chem. Res.*, vol. 40, no. 23, pp. 5246–5254, 2001.

[46] Y. Shi *et al.*, "Pore engineering of hierarchically structured hydrodemetallization catalyst pellets in a fixed bed reactor," *Chem. Eng. Sci.*, vol. 202, pp. 336–346, Jul. 2019, doi: 10.1016/j.ces.2019.03.049.

[47] J. J. Meyers and A. I. Liapis, "Network modeling of the convective flow and diffusion of molecules adsorbing in monoliths and in porous particles packed in a chromatographic column," *J. Chromatogr. A*, vol. 852, no. 1, pp. 3–23, Aug. 1999, doi: 10.1016/S0021-9673(99)00443-4.

[48] C. Jungreuthmayer *et al.*, "The 3D pore structure and fluid dynamics simulation of macroporous monoliths: High permeability due to alternating channel width," *J. Chromatogr. A*, vol. 1425, pp. 141–149, Dec. 2015, doi: 10.1016/j.chroma.2015.11.026.

[49] J. J. Meyers and A. I. Liapis, "Network modeling of the intraparticle convection and diffusion of molecules in porous particles packed in a chromatographic column," *J. Chromatogr. A*, vol. 827, no. 2, pp. 197–213, Dec. 1998, doi: 10.1016/S0021-9673(98)00658-X.

[50] J. H. Petropoulos, J. K. Petrou, and A. I. Liapis, "Network model investigation of gas transport in bidisperse porous adsorbents," *Ind. Eng. Chem. Res.*, vol. 30, no. 6, pp. 1281–1289, Jun. 1991, doi: 10.1021/ie00054a031.

[51] P. Kočí, F. Štěpánek, M. Kubíček, and M. Marek, "Modelling of micro/nano-scale concentration and temperature gradients in porous supported catalysts," *Chem. Eng. Sci.*, vol. 62, no. 18–20, pp. 5380–5385, Sep. 2007, doi: 10.1016/j.ces.2006.12.033.

[52] P. Kočí, V. Novák, F. Štěpánek, M. Marek, and M. Kubíček, "Multi-scale modelling of reaction and transport in porous catalysts," *Chem. Eng. Sci.*, vol. 65, no. 1, pp. 412–419, Jan. 2010, doi: 10.1016/j.ces.2009.06.068.

[53] W. Ribeiro Do Prado Júnior, J. A. Martins, and E. C. Romão, "Utilizing Numerical Simulations to Analyze the Efficiency of a Porous Reactor," *Eng. Technol. Appl. Sci. Res.*, vol. 12, no. 3, pp. 8755–8759, Jun. 2022, doi: 10.48084/etasr.4957.

[54] J.-L. Auriault, "On the Domain of Validity of Brinkman's Equation," *Transp. Porous Media*, vol. 79, no. 2, pp. 215–223, Sep. 2009, doi: 10.1007/s11242-008-9308-7.

[55] S. I. Vasin and A. N. Filippov, "Permeability of complex porous media," *Colloid J.*, vol. 71, no. 1, pp. 31–45, Feb. 2009, doi: 10.1134/S1061933X09010049.

[56] W. Yao, Y. Li, and N. Chen, "Analytic solutions of the interstitial fluid flow models," *J. Hydrodyn.*, vol. 25, no. 5, pp. 683–694, Oct. 2013, doi: 10.1016/S1001-6058(13)60413-8.

[57] S. B. Ameur, C. Luminiţa Gîjiu, M.-P. Belleville, J. Sanchez, and D. Paolucci-Jeanjean, "Development of a multichannel monolith large-scale enzymatic membrane and application in an immobilized enzymatic membrane reactor," *J. Membr. Sci.*, vol. 455, pp. 330–340, Apr. 2014, doi: 10.1016/j.memsci.2013.12.026.

[58] A. Ciemięga, K. Maresz, J. Malinowski, and J. Mrowiec-Białoń, "Continuous-Flow Monolithic Silica Microreactors with Arenesulphonic Acid Groups: Structure–Catalytic Activity Relationships," *Catalysts*, vol. 7, no. 9, p. 255, Aug. 2017, doi: 10.3390/catal7090255.